Emodin attenuated severe acute pancreatitis via the P2X ligand-gated ion channel 7/NOD-like receptor protein 3 signaling pathway

QINGKAI ZHANG[1], XUFENG TAO[2], SHILIN XIA[3], JIALIN QU[3], HUIYI SONG[3], JIANJUN LIU[3], HAILONG LI[4] and DONG SHANG[1,5]

[1]Department of Integrative Medicine Surgery, Dalian Medical University, Dalian, Liaoning 116011; [2]Department of Pharmacology, Dalian Medical University, Dalian, Liaoning 116044; [3]Department of General Surgery, The First Affiliated Hospital of Dalian Medical University, Dalian, Liaoning 116011, P.R. China; [4]Department of Psychology, University of South Carolina, Columbia, SC 29208, USA; [5]Department of General Surgery, The First Affiliated Hospital of Dalian Medical University, Dalian, Liaoning 116011, P.R. China

Received June 15, 2018; Accepted October 26, 2018

DOI: 10.3892/or.2018.6844

Abstract. Acute pancreatitis (AP) is an aseptic inflammation characterized with an annual incidence rate, and ~20% patients progressing to severe AP (SAP) with a high mortality rate. Although Qingyi decoction has been frequently used for SAP treatment over the past 3 decades in clinic, the actual mechanism of its protective effects remains unknown. As the major active ingredient of Qingyi decoction, emodin was selected in the present study to investigate the effect of emodin against severe acute pancreatitis (SAP) in rats through NOD-like receptor protein 3 (NLRP3) inflammasomes. The rats were randomly divided into a sham operation group, an SAP model group induced by a standard retrograde infusion of 5.0% sodium taurocholate into the biliopancreatic duct, and low-dose (30 mg/kg) and high-dose (60 mg/kg) emodin-treated groups. At 12 h after the event, the plasma amylase, lipase, interleukin (IL)-1β, IL-18 and myeloperoxidase (MPO) activities were examined. Furthermore, the pathological scores of pancreases were evaluated by hematoxylin and eosin staining. The expression levels of P2X ligand-gated ion channel 7 (P2X7), NLRP3, apoptosis-associated speck-like protein containing a C-terminal caspase recruitment domain and caspase-1 were also analyzed by western blot analysis. The data demonstrated that, compared with the SAP group, emodin could significantly relieve the pancreatic histopathology and acinar cellular structure injury, and notably downregulate the plasma amylase and lipase levels, as well as the MPO activities in pancreatic tissues, in a dose-dependent manner. Furthermore, emodin inhibited the P2X7/NLRP3 signaling pathway followed by the decrease of pro-inflammatory factors, and the latter is beneficial for the recovery of SAP. Collectively, the data indicated that emodin may be an efficient candidate natural product for SAP treatment.

Correspondence to: Dr Dong Shang, Department of General Surgery, The First Affiliated Hospital of Dalian Medical University, Dalian, Liaoning 116011, P.R. China
E-mail: shangdong@dmu.edu.cn

Dr Hailong Li, Department of Psychology, University of South Carolina, 915 Green Street, Discovery Building, RM 324, Columbia, SC 29208, USA
E-mail: hailong@mailbox.sc.edu

Key words: acute pancreatitis, emodin, P2X ligand-gated ion channel 7, NOD-like receptor protein 3, inflammation

Introduction

As one of the most common gastrointestinal diseases, acute pancreatitis (AP) frequently occurs due to gallstones and alcohol abuse, with an annual incidence rate of 13-45/100,000 in USA in 2011 (1). Although 80% of patients with AP exhibit mild symptoms, including abdominal pain, fever, nausea and vomiting, ~20% of patients with AP progress to severe AP (SAP), which has a mortality rate of 20-40% in USA in 2005 (2,3). Furthermore, patients with SAP frequently develop specific chronic diseases following being discharged from hospital, including prediabetes, diabetes, chronic pancreatitis and pancreatic cancer (4,5). At present, the primary treatment for SAP is limited to supportive care and treatment of complications (2). However, there are only a limited number of drugs available, and the efficiency is not satisfactory (6,7). Therefore, the investigation of an effective drug or other therapeutic options is critical for the treatment of SAP in clinic.

SAP begins with premature activation of digestive enzymes within the pancreatic acinar cell, which can cause acinar cell necrosis and subsequent activation of the pro-inflammatory cascade, resulting in systemic inflammatory response syndrome as well as multiple organ dysfunctions (1,8). Numerous studies demonstrated that the extent of inflammatory response positively associates with disease severity;

however, the detailed molecular mechanisms remain unclear (9,10). Proinflammatory cytokines from activated monocytes and macrophages, including interleukin (IL)-1β and IL-18, are hypothesized to have an important function in this cascade (11). Thus, an improved understanding of IL-1β and IL-18 synthesis and secretion is beneficial for the development of novel anti-SAP drugs. Recent studies have been directed to the purinergic receptor P2X ligand-gated ion channel 7 (P2X7), which serves a key role in the maturation of IL-1β and IL-18 through the recruitment of the NOD-like receptor protein 3 (NLRP3) inflammasome-caspase-1 complex (12-14). The positive association between the severity of SAP and pro-inflammatory cascade indicates that the P2X7/NLRP3 signaling pathway could be a reliable therapeutic target for SAP (9).

Emodin is a natural anthraquinone compound from the oriental herb *Rheum officinale* Baill, which has various physiological effects, particularly its anti-inflammatory properties (15). It is also the primary active ingredient of Dachengqi decoction and Qingyi decoction that have been frequently used for SAP treatment (16-19). However, the potential therapeutic mechanism is not fully understood. Previous studies provide evidence for a novel role of emodin as an antagonist of P2X7R, which can inhibit ATP-induced IL-1β secretion from rat peritoneal macrophages through the inhibition of P2X7R activation (20-22). Han *et al* (23) determined the effects of emodin on inflammation-associated disorders, including endotoxemia, Alzheimer's disease, obesity and fibromyalgia through the regulation of NLRP3 inflammasome activation (25,26). In the present study, the effects of emodin on regulating the P2X7/NLRP3 signaling pathway whilst the SAP rat model was induced by intraductal infusion of 5.0% sodium taurocholate, and the functions and mechanisms for its protective effects were investigated.

Materials and methods

Reagents and materials. Emodin (cat. no. IE0070) and sodium taurocholate (cat. no. T8510) was obtained from Solarbio Science & Technology Co., Ltd. (Beijing, China). Rat IL-18 ELISA kit (cat. no. ab213909), rat IL-1β ELISA kit (cat. no. ab100768), rat Pancreatic Amylase ELISA kit (cat. no. ab137969) and rat Lipase ELISA kit (cat. no. ab102524) were obtained from Shanghai Lengton Bioscience Co., Ltd. (Shanghai, China). The Power Vision Two-Step histo-staining reagent (cat. no. I003-1) was purchased from Nanjing Jiancheng Bioengineering Institute (Nanjing, China). A BCA protein assay kit (cat. no. P0010S) was purchased from Beyotime Institute of Biotechnology (Shanghai, China). Rabbit anti-P2X7 (1:1,000, cat. no. 1114-1-AP), caspase-1 (1:1,000, cat. no. 22915-1-AP) and myeloperoxidase (MPO; 1:100, cat. no. 22225-1-AP), GAPDH-conjugated Affinipure IgG (1:800, cat. no. 10494-1-AP), horseradish peroxidase-conjugated goat anti-rabbit IgG (1:300, cat. no. SA00001-2) and tetramethylrhodamine (TRITC)-conjugated goat anti-rabbit IgG (H+L) (1:300, cat. no. SA00007-2) were purchased from Proteintech Group, Inc. (Chicago, IL, USA). Rabbit anti-NLRP3 (1:1,000, cat. no. bs-6655R) and rabbit anti-apoptosis-associated speck-like protein containing a C-terminal caspase recruitment domain (ASC) (1:1,000, cat. no. bs-6741R) were purchased from Biosynthesis Biotechnology Co., Ltd. (Beijing, China). All antibodies were diluted in TBST buffer (20 mM Tris-HCl, 500 mM NaCl and 0.05% Tween-20; pH 7.5).

Experimental animals. A total of 48 male Sprague-Dawley (SD) rats with body weight 250±20 g were obtained from the Experimental Animal Center of Dalian Medical University (Dalian, China). SD rats were kept at 21±2˚C with 50±10% relative humidity and a 12/12 h light/dark cycle, with free access to standard laboratory feed and water. The experimental protocol was approved by the Ethical Committee for Laboratory Animal Care and Use of Dalian Medical University.

Animal model. SD rats were randomly divided into 4 groups (n=12), including: Sham operation (SO); SAP model (SAP); and low-dose (30 mg/kg) and high-dose (60 mg/kg) emodin-treated groups. SAP was induced according to our previously described method (19). Briefly, rats were anesthetized with 2.5% sevoflurane in an induction chamber following fasting for 12 h. Subsequently, the pancreas was exposed along a midline incision. The biliopancreatic duct was cannulated through the duodenum, and the hepatic duct was closed by a microvascular clamp, temporarily. Following this, SAP was induced by a standard retrograde infusion of 5.0% sodium taurocholate (0.1 ml/100 g body weight) into the biliopancreatic duct. Finally, the pancreas was carefully replaced and the abdomen was closed. The SO group was administered with sterile saline. Additionally, emodin was suspended in 0.5% sodium carboxymethylcellulose (CMC-Na). Emodin was intra-gastrically applied to the rats immediately and at 6 h after the administration of sodium taurocholate. The SO and SAP groups were administered with 0.5% CMC-Na of equivalent volume. Samples were obtained at 12 h after the model was established. Blood samples were obtained for biochemical analyses. The pancreatic head was fixed with 10% formalin for 24 h at room temperature and embedded in paraffin for histopathological examination. For western blot analyses, pancreas samples were immediately frozen and maintained at -80˚C.

Plasma amylase and lipase assays. Plasma amylase and lipase levels were assayed with commercially available rat Pancreatic Amylase ELISA kit and rat Lipase ELISA kit, according to the manufacturer's protocols. The absorbance at 450 nm representing the relative level of amylase and lipase in each well was measured by a microplate reader purchased from Thermo Fisher Scientific, Inc. (Waltham, MA, USA).

Histopathological examination. Formalin-fixed tissue samples from each group were sliced (5 μm), dewaxed and stained with hematoxylin and eosin (H&E) for histological examination (hematoxylin for 5 min and 0.5% eosin for 3 min) at 37˚C. Images were captured using a light microscope (Leica DM4000B; Leica Microsystems GmbH, Wetzlar, Germany) at x200 magnification. The pathological scores were evaluated based on the scoring system detailed in Table I (16).

Transmission electron microscope assay. A small portion of pancreas (<1 mm^3) were fixed overnight at 4˚C in 2% glutaraldehyde, followed by postfixed with 1% osmium tetroxide for 2 h at 4˚C after washing 3 times (15 min/time) in 0.1 M

Table I. Histological scoring for acute pancreatitis.

Condition	Score	Description
	0	Absent
	1	Focally increased between lobules (localized enlargement of the pancreas secondary to interstitial or inflammatory edema without necrosis)
Edema	2	Diffusely increased between lobules
	3	Acini disrupted and separated
	4	3 + diffuse expansion in intercellular septas
	0	Absent
	1	Around ductal margin
Inflammation	2	In parenchyma (<50% of lobules)
	3	In parenchyma (51-75% of lobules)
	4	In parenchyma (>75% of lobules)
Vacuolization	0	Absent
	1	Periductal (<5%)
	2	Focal (5-20%)
	3	Diffuse (21-50%)
	4	Severe (>50%)

The samples were evaluated by a pathologist blind to the study groups under a light microscopy. Edema, inflammation, and vacuolization in pancreatic tissue were scored between 0 and 4.

sodium cacodylate buffer (cat. no. 97068, Sigma-Aldrich; Merck KGaA, Darmstadt, Germany). Subsequently, tissues were dehydrated in 50, 70, 95 and 100% ethanol solutions (15 min per concentration) and embedded in epoxyresin. Ultrathin sections were sliced (70 nm) and collected on copper grids. The obtained sections were stained with uranyl acetate (2 h at room temperature) and lead citrate (5 min at room temperature), and then observed using a JE-2000EX transmission electron microscope (JEOL Ltd, Tokyo, Japan) at x12,000 magnification.

Immunohistochemical detection of MPO. The Power Vision Two-Step Histo-staining Reagent was used to determine the MPO expression in the pancreas. Briefly, at room temperature, tissue sections (5 μm) of 10% formalin-fixed samples in each group were dewaxed in xylene (10 min) and 50, 70, 95 and 100% ethanol (5 min each) and washed 3 times in tap water. Endogenous peroxidase activity was blocked with 3% (v/v) H_2O_2, and the sections were incubated with 5% bovine serum albumin for 10 min at room temperature. Rabbit polyclonal anti-MPO antibody (1:100) was incubated overnight at 4˚C. Subsequently, sections were washed with PBS 3 times for 15 min and incubated with horseradish peroxidase-conjugated goat anti-rabbit IgG (1:300) for 1 h at 37˚C. Images were captured with a light microscope (Leica DM4000B) at x200 magnification. Integral optic density (IOD) of the images was counted using Image Pro Plus 6.0 software (Media Cybernetics, Inc., Rockville, MD, USA).

Immunofluorescence detection of MPO. Immunofluorescence staining of MPO was performed with pancreas sections as described by Liu *et al* (20). The sections were dewaxed in a gradient of ethanol (50, 70, 95 and 100%; 5 min per concentration) at room temperature, and blocked with 5% bovine serum albumin for 20 min at room temperature following washing 3 times with PBS (5 min/time). Subsequently, the slides were treated with rabbit polyclonal anti-MPO antibodies (1:100) at 37˚C for 2 h, and then incubated with TRITC-conjugated goat anti-rabbit IgG (H+L) (1:300) for 1 h at room temperature in the dark. Digital images were captured with an Olympus BX63 fluorescent microscope (Olympus BX63; Olympus Corporation, Tokyo, Japan) at x200 magnification. Fluorescent intensity of the images was calculated using Image Pro Plus 6.0 software.

Western blotting assay. Total protein was extracted from the pancreas tissues in different groups using a whole protein extraction kit (Nanjing KeyGen Biotech Co., Ltd., Nanjing, China), and the protein concentration was assayed using a BCA protein assay kit. Samples (50 μg) were separated by 10% SDS-PAGE and transferred onto polyvinylidene fluoride membranes. The blots were blocked with 5% non-fat milk at room temperature for 3 h, and then incubated overnight at 4˚C with the primary antibodies against P2X7, NLRP3, ASC and caspase-1 (1:1,000 dilution). Subsequently, the blots were incubated with the horseradish peroxidase-conjugated goat anti-rabbit IgG (1:1,000) for 4 h at room temperature. Proteins were detected by BeyoECL Plus enhanced chemiluminescence substrate (cat. no. P0018; from Beyotime Institute of Biotechnology). Protein bands were visualized with a ChemiDoc XRS bioimaging system (Bio-Rad Laboratories, Inc., Hercules, CA, USA). Bands were normalized with GAPDH (1:800 dilution with TBST buffer) as an internal control.

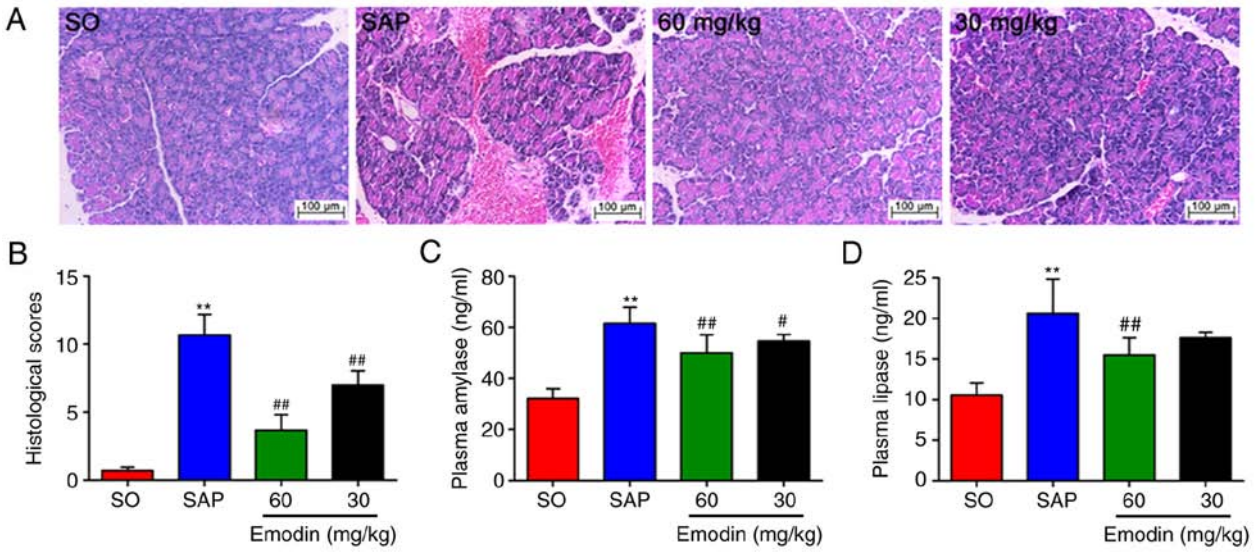

Figure 1. Emodin alleviates pancreatic injury in SAP rats. (A) Effects of emodin on hematoxylin and eosin staining of the pancreas in SAP rats. Images are depicted at x200 magnification (n=3). (B) The histological scores of the pancreases in SAP rats. (C) Effects of emodin on the plasma levels of amylase in SAP rats. (D) Effects of emodin on the plasma levels of lipase in SAP rats. The data are presented as the mean ± standard deviation, n=12. **P<0.01 vs. SO; $^{\#}$P<0.05 vs. SAP and $^{\#\#}$P<0.01 vs. SAP. SAP, severe acute pancreatitis; SO, sham operation.

Plasma IL-1β and IL-18 assay. Plasma IL-1β and IL-18 levels were detected by Rat IL-18 ELISA kit and rat IL-1β ELISA kit (cat. no. ab100768), according to the manufacturer's protocols. Briefly, the plasma in each group was transferred into a 96-well plate with a coating layer of IL-1β and IL-18 antibodies, and incubated at 37˚C for 60 min. Following this, the plate was washed 5 times with diluted washing solution. Subsequently, the chromogen solution and stop solution was sequentially added into each well for incubation of 10 min at room temperature in the dark. Finally, the absorbance at 450 nm in each well was measured by a microplate reader (Thermo Fisher Scientific Inc.). The standard curve was established to calculate the concentration of IL-1β and IL-18.

Statistical analysis. All statistical analyses were performed using SPSS 17.0 software (SPSS, Inc., Chicago, IL, USA). Data are expressed as the mean ± standard deviation. The differences between the groups were analyzed using one-way analysis of variance with the least significance difference test. P<0.05 was considered to indicate a statistically significant difference.

Results

Emodin alleviates pancreatic injury in SAP rats. As depicted in Fig. 1A and B, there were no distinct pathological changes in the SO group, whereas H&E staining results revealed that pancreatic injury in SAP rats contained large areas of tissue edema, together with leukocyte infiltration, acinar cell vacuolization, necrosis and hemorrhage, and the histological scores were significantly increased (P<0.01, SAP vs. SO). However, alleviated pancreatic injury and decreased pancreatic histological scores were observed in the emodin-treated groups, particularly in the high-dose (60 mg/kg) group (P<0.01; Emodin 60 mg/kg vs. SAP).

To examine the effect of emodin on the severity of SAP, the activities of plasma amylase and lipase were examined using ELISA kits. The results confirmed that the plasma amylase and lipase levels in the SAP group were 2-fold increased, compared with the SO group (P<0.01). However, the application of emodin notably downregulated these elevations in a dose-dependent manner (Fig. 1C and D; P<0.01, Emodin 60 mg/kg vs. SAP). These results indicated the beneficial effects of emodin on pancreatic injury in SAP rats.

Emodin attenuates acinar cellular structure injury in SAP rats. The detailed characterization of ultrastructural changes in rat pancreatic acinar cells following SAP injury was observed with transmission electron microscope technology at x12,000 magnification. Electron micrography of acinar cells in the SO group demonstrated a regular cellular structure with a rough endoplasmic reticulum (RER)-rich basal region (Fig. 2A). However, in the SAP group, focal dilation and degranulation of RER was observed in acinar cells, with an accumulation of autophagic vacuoles and dense materials. Additionally, notable damage to the solitary mitochondria and widespread blebbing of the cytoplasm were observed in the basal zones of acinar cells (Fig. 2B; black arrow). Treatment with emodin notably ameliorated acinar cellular structure injury in a dose-dependent manner (Fig. 2D and C). These results further demonstrated that emodin possessed a potent protective effect on the ultrastructure of acinar cells following inducing SAP damage.

Emodin downregulates the expression levels of MPO in the pancreatic tissue of SAP rats. MPO content is considered as the indicator of local neutrophil sequestration in the pancreas following inducing SAP (21). In the present study, the images of immunohistochemical analysis indicated that the rats in the SAP group exhibited an increased MPO-positive area in the

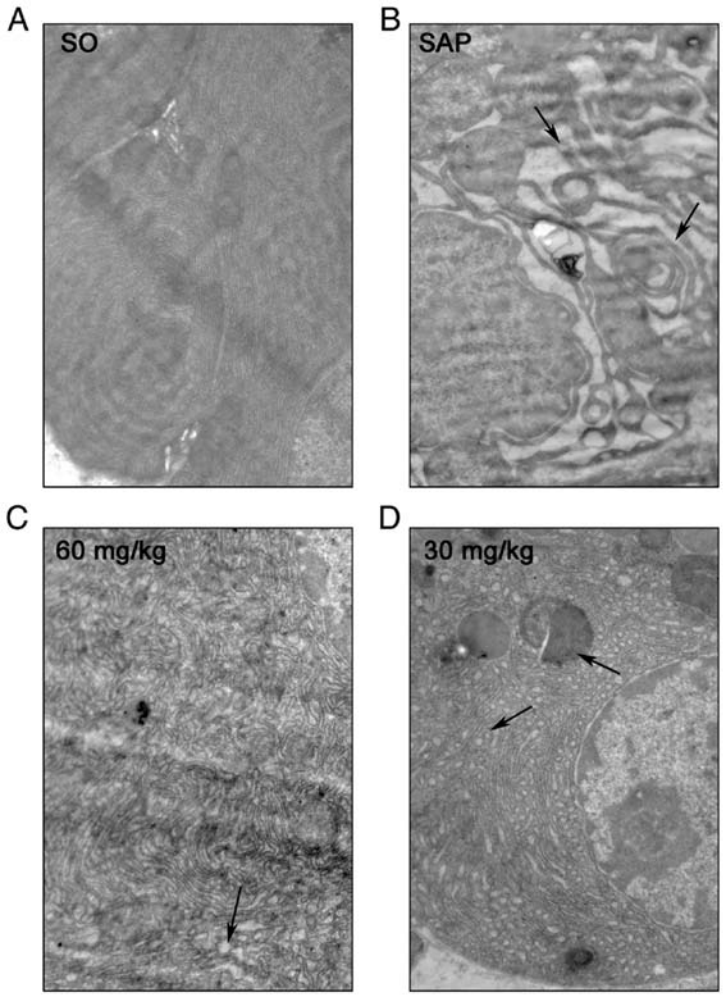

Figure 2. Emodin attenuates acinar cellular structure injury in SAP rats. Representative images of cell ultrastructure in the (A) SO, (B) SAP, (C) high-dose emodin-treated (60 mg/kg) and (D) low-dose emodin-treated groups. Images were depicted at x12,000 magnification, n=3. Black arrow indicate granular cytoplasmic reticulum, and adverse changes in the solitary mitochondria and cytoplasmic vacuoles in acinar cells. SAP, severe acute pancreatitis; SO, sham operation.

pancreas, compared with the SO group. Following emodin treatment, the protein expression of MPO was significantly decreased [P<0.01, Emodin (60 or 30 mg/kg) vs. SAP; P<0.05, Emodin 30 mg/kg vs. SAP], thereby downregulating IOD in a dose-dependent manner, compared with the SAP group (Fig. 3A and B).

Furthermore, immunofluorescence indicated that MPO activity was significantly increased following the induction of SAP. Emodin administration could notably downregulate pancreatic MPO expression, as manifested by the reduced fluorescence intensity, compared with the SAP group [Fig. 3C and D; P<0.01, Emodin (60 or 30 mg/kg) vs. SAP]. These data indicated that emodin could decrease neutrophil infiltration into the pancreas and block the inflammation cascade.

Emodin inhibits the expression of P2X7/NLRP3 pathway-associated proteins in pancreatic tissues. In the present study, whether the P2X7/NLRP3 signaling pathway is involved in the protective effects of emodin on SAP in rats was investigated. As depicted in Fig. 4A-D, the expression levels of P2X7, NLRP3, ASC and caspase-1 in the pancreatic tissue were significantly increased (P<0.01, SAP vs. SO) Furthermore, treatment with emodin (30 mg/kg) inhibited the expression levels of P2X7, NLRP3, ASC and caspase-1, but the difference was not statistically significant (P>0.05, Emodin 30 mg/kg vs. SAP). However, these inhibitions were significant in the high-dose emodin-treated (60 mg/kg) group (P<0.01, Emodin 60 mg/kg vs. SAP). The western blot results indicated that emodin inhibited the P2X7/NLRP3-mediated signaling pathway.

Emodin reduces the plasma concentrations of IL-1β and IL-18. The *in vivo* effects of emodin on IL-1β and IL-18 release was also investigated. As depicted in Fig. 5A and B, compared with the SO group, the plasma levels of the IL-1β and IL-18 were significantly increased following the SAP event (P<0.01, SAP vs. SO), which were reduced when emodin (60 mg/kg) was administered (P<0.01, Emodin 60 mg/kg vs. SAP). The levels of these 2 pro-inflammatory cytokines were reduced in the low-dose emodin-treated group, but this was not statistically significant, while this reduction was significantly decreased in the high-dose emodin-treated group (P<0.01, Emodin 60 mg/kg vs. SAP).

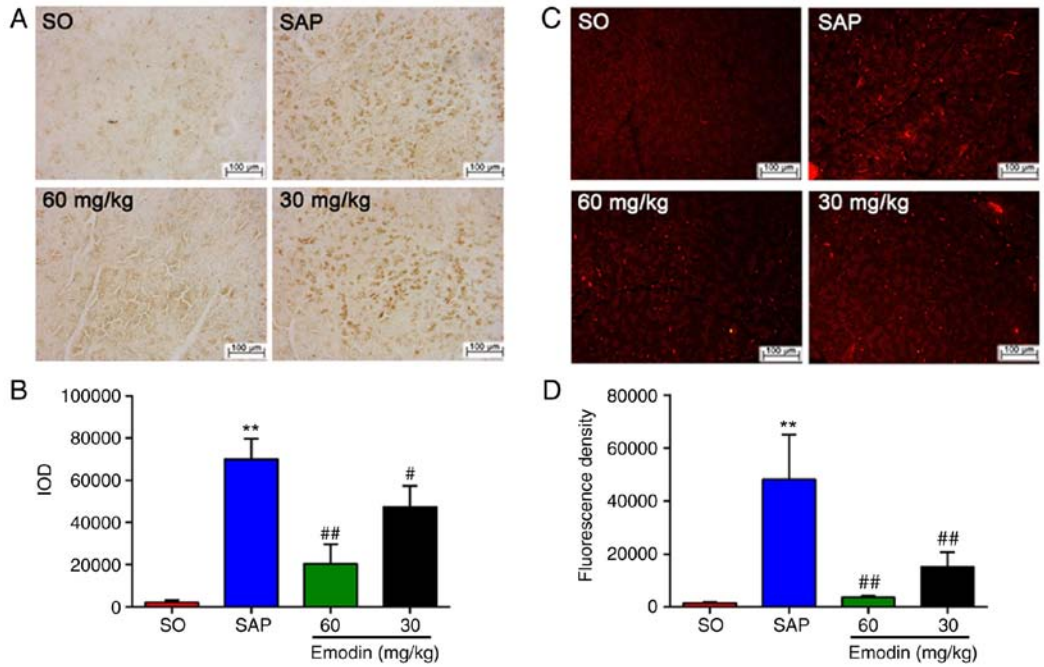

Figure 3. Emodin downregulates the expression of MPO in the pancreas of rats with SAP. (A) Effects of emodin on MPO-immunopositive (brown) staining region of the pancreas in SAP rats using an immunohistochemical assay (n=6). Images were depicted at x20 magnification. (B) The IOD of the immunohistochemical images. (C) Effects of emodin on MPO-immunopositive (red) staining region of the pancreas in SAP rats using an immunofluorescence assay (n=6). Images were depicted at x20 magnification. (D) The fluorescence density of the immunofluorescence images. The data are presented as the mean ± standard deviation. **P<0.01 vs. SO, $^{\#}$P<0.05 vs. SAP and $^{\#\#}$P<0.01 vs. SAP. SAP, severe acute pancreatitis; SO, sham operation; MPO, myeloperoxidase; IOD, integral optic density.

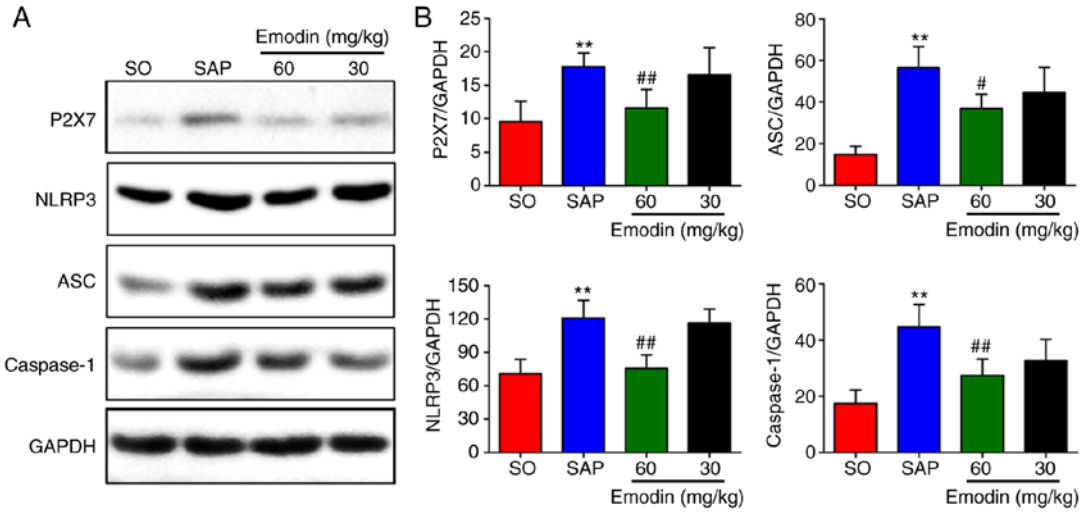

Figure 4. Emodin inhibits the expression of P2X7 and NLRP3 in the pancreatic tissues. (A) Effects of emodin on the protein expression of P2X7, NLRP3, ASC and caspase-1 in SAP rats. (B) Statistical analysis of the effects of emodin on proteins expression levels (n=3). The data are presented as the mean ± standard deviation, **P<0.01 vs. SO, $^{\#}$P<0.05 vs. SAP and $^{\#\#}$P<0.01 vs. SAP. SAP, severe acute pancreatitis; SO, sham operation; P2X7, P2X ligand-gated ion channel 7; NLRP3, NOD-like receptor protein 3; ASC, apoptosis-associated speck-like protein containing a C-terminal caspase recruitment domain.

Discussion

SAP is a common clinical condition with high incidence of morbidity and mortality due to the lack of effective medicine against this disease (1,2). Therefore, novel drugs with high efficacy and minimal side effects are vital for SAP treatment. Studies have indicated that emodin is a potential candidate in the treatment of clinical and experimental SAP, but the underlying mechanisms by which emodin performs its pharmacological activities, particularly on anti-inflammatory effects during SAP, remain unknown (18,19,27).

Pancreatic histopathological alterations, including interstitial edema, inflammatory cell infiltration and acinar cell vacuolization, are the crucial alterations for evaluating pancreatic damage (19). In the present experiments, the classic rat model of SAP induced by intraductal infusion of 5.0% sodium taurocholate was used and it was demonstrated that emodin may improve SAP-induced histopathological

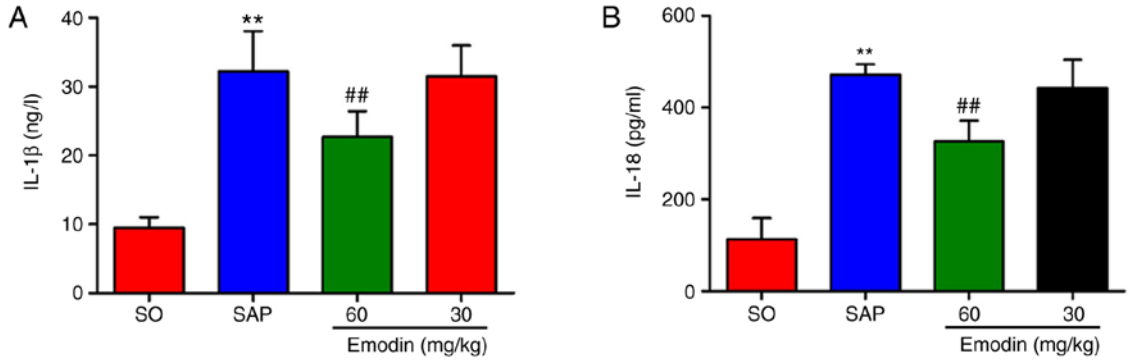

Figure 5. Emodin reduces the plasma concentration of IL-1β and IL-18. (A) Effects of emodin on the plasma concentration of IL-1β in SAP rats. (B) Effects of emodin on the plasma concentration of IL-18 in SAP rats. The data were presented as the mean ± standard deviation. **P<0.01 vs. SO and $^{\#\#}$P<0.05 vs. SAP. IL, interleukin; SAP, severe acute pancreatitis; SO, sham operation.

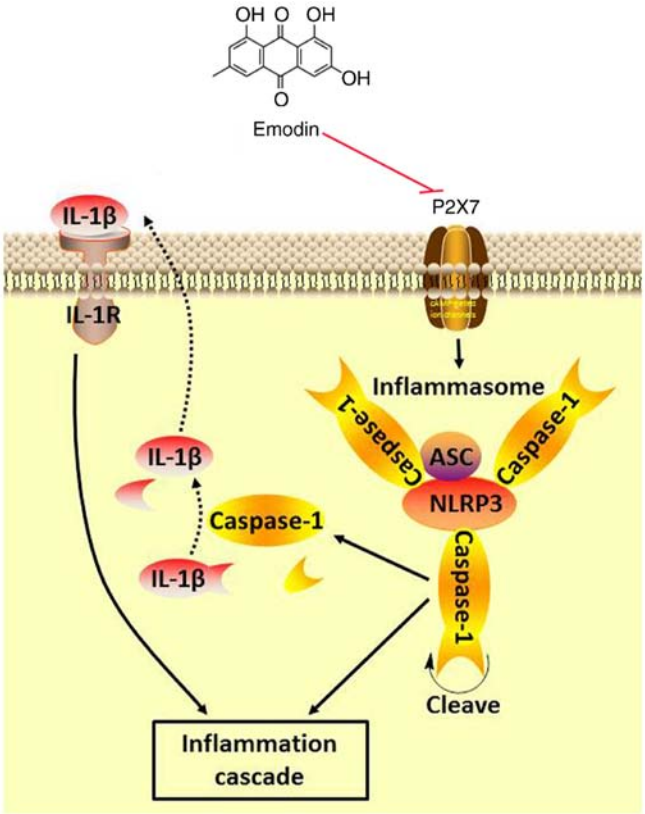

Figure 6. The schematic model for the protection of emodin against acute pancreatitis in rats via inhibiting the P2X7/NLRP3 signaling pathway. IL, interleukin; P2X7, P2X ligand-gated ion channel 7; NLRP3, NOD-like receptor protein 3; ASC, apoptosis-associated speck-like protein containing a C-terminal caspase recruitment domain.

and ultrastructural alterations in a dose-dependent manner. According to the Atlanta classification and definitions, pancreatic digestive enzymes, including amylase and/or lipase, are the most common biochemical hallmarks of SAP (8). Additionally, treatment with emodin may decrease plasma amylase and lipase levels as well as MPO activities in pancreatic tissues of SAP rats.

SAP is an aseptic inflammation characterized by a large number of pro-inflammatory cytokines released from damaged acinar cells (11). P2X7, as a member of the P2X family of ATP-gated cation channels, is an important molecule in inflammation (28). It has a long (250 amino acid) intracellular C-terminal domain, which enables the coupling of channel activation to a complex and diverse downstream signaling cascade (12). The activation of P2X7 stimulates multiple signaling pathways, including reactive oxygen species (ROS) and mitogen-activated protein kinase, and nuclear factor (NF)-κB transcription factors, with the latter producing a large number of inflammatory mediators (29-31). Recent studies demonstrated that P2X7 activation is one of the most effective stimuli for NLRP3 inflammasome activation (12,32,33). The NLRP3 inflammasome is a macromolecular multiprotein complex with a molecular weight of ~700 kDa, which composes of NLRP3, adaptor protein ASC and effector protein caspase-1 (34). NLRP3 is one of the members of the NOD-like receptor family of cytoplasmic recognition receptors that recognizes intrinsic hazards and external stress signals, including ATP and ROS (35). As a core protein, activated NLRP3 recruits downstream proteins ASC and caspase-1 to form the NLRP3 inflammasome (36). Following the assembly, the inactive caspase-1 precursor is activated into caspase-1, which promotes cleavage, maturation and release of inactivated pro-IL-1β and pro-IL-18, and induces the inflammatory cascade (37). Studies demonstrated that NLRP3 can also increase the expression of IL-1β precursor by activating the NF-κB signaling pathway and further enhance the effect of the NLRP3 inflammasome (21,22,38). To investigate whether the protective functions of emodin administration derived from the P2X7/NLRP3 signaling pathway, the expression levels of P2X7, NLRP3, ASC and caspase-1 in pancreatic tissues were examined. It was determined that all 4 protein expression levels were significantly enhanced in the SAP group, compared with the SO group, indicating that the P2X7/NLRP3 signaling pathway-associated proteins participated in SAP, while the expression levels of these 4 proteins were decreased following emodin administration (vs. SAP). This indicated that the protective effects of emodin against SAP may be partially through inhibiting the activation of P2X7 and NLRP3 inflammasome. Numerous studies demonstrated that P2X7R is primarily expressed in rodent duct cells in the pancreas, which regulates calcium signaling and ion transport (13,14,39). Notably, Novak *et al* (40) demonstrated that the P2X7 receptors are also expressed in exocrine glands. The acini in the pancreas exhibits low functionality of purinergic

receptor signaling and apparent lack of P2X7 receptors, but the pancreatic duct cells highly expressed various P2 receptors, particularly P2X7 receptors (40). Additionally, the initial injury in SAP is characteristically sterile, which results in acinar cells necrosis (41). Furthermore, the sterile inflammatory response mediated through damage associated molecular patterns (DAMPs) released from necrotic acinar cells serve a vital role in the process of pancreatic injury, which functions through the plasma membrane P2X7 receptor (42). Further studies will focus on the regulating effect of emodin on the DAMPs system in SAP. Additionally, based on the present data, the P2X7/NLRP3 mediated inflammatory signaling pathway was activated at 12 h after the event. However, inflammation primarily depends on the time-course, which indicated that P2X7 induction would be associated with the severity of pancreatitis. This is an notable expectation for P2X7 research in pancreatitis in the future.IL-1β and IL-18 are important pro-inflammatory cytokines regulated by the NLRP3 inflammasome, and serve a central role in the regulation of inflammation and innate immune system during inflammatory diseases, including Crohn's disease and Blau syndrome (12,43). IL-1β is considered to be one of the earliest and most potent pro-inflammatory factors synthesized and released in response to infectious and injuries, and therefore it is significant to septic and sterile inflammation (11,44). Previous studies demonstrated that IL-1β is associated with the severity of SAP, and inhibition of IL-1β can relieve SAP (45,46). Mature IL-1β binds to IL-1β receptors to regulate the modification and activation of proinflammatory cytokines, including tumor necrosis factor (TNF)-α, IL-8 and IL-17 (47). IL-18 is a novel pro-inflammatory cytokine with a similar structure and function to IL-1β (48). Recently, numerous studies focused on the important roles that IL-18 serves in the synthesis and secretion of IL-1, TNF-α and other chemokines (12,23). Therefore, blocking the overproduction of these proinflammatory factors indicates a potential efficient route for SAP therapy.

In the present study, the levels of plasma IL-1β and IL-18 following emodin treatment were analyzed. Results demonstrated that the levels of IL-1β and IL-18 in the SAP group were significantly increased, compared with the SO group, while they were slightly reduced in the low-dose emodin-treated group, but notably decreased in the high-dose emodin-treated group. This indicated a potential suppression function of emodin on the P2X7/NLRP3 signaling pathway. The rat model that was used in the present study is a typical model of SAP (24). According to our previous studies, at 6 h after the induction, the rat exhibited a notable increase of inflammatory level, which could mimic the clinic characteristics of patients with SAP. Therefore, using the 6 h time point for the administration of emodin would provide the highest beneficial effects (24,49). In conclusion, the anti-inflammatory effect of emodin on SAP rats may reduce the concentration of IL-1β and IL-18 in plasma by inhibiting the P2X7/NLRP3 signaling pathway, thereby delaying the progress of SAP and improving the systemic inflammatory status (Fig. 6). Therefore, emodin is expected to be one of the emerging and efficient candidate natural products for SAP treatment. However, it requires further clinical investigations on the positive effects of emodin based on routine treatment and to determine how to inhibit inflammatory responses in the early stages of SAP.

Acknowledgements

The authors would like to thank Dr Hong Xiang (Department of Integrative Medicine Surgery, Dalian Medical University, Dalian, China) for data analysis and Figure revision.

Funding

This study was supported by the National Natural Science Foundation of China (grant no. 81373875) and the Key Project Supported by Clinical Ability Construction of Liaoning Province (grant no. LNCCC-A03-2015).

Availability of data and materials

The datasets used and/or analyzed during the present study are available from the corresponding author on reasonable request.

Authors' contributions

QZ and XT performed the experiment and the data analysis. DS and HL drafted the manuscript, designed the experiment and revised the manuscript. SX, JQ, HS and JL performed the immunostaining, transmission electron microscopy and western blot analysis assay. All authors read and approved the final manuscript.

Ethics approval and consent to participate

The experimental protocol was approved by the Ethical Committee for Laboratory Animal Care and Use of Dalian Medical University.

Patient consent for publication

Not applicable.

Competing interests

The authors declare that they have no conflict of interest.

References

1. Lankisch PG, Apte M and Banks PA: Acute pancreatitis. Lancet 386: 85-96, 2015.
2. Tenner S, Baillie J, DeWitt J and Vege SS; American College of Gastroenterology: American college of gastroenterology guideline: Management of acute pancreatitis. Am J Gastroenterol 108: 1400-1415; 2013.
3. Ince AT and Baysal B: Pathophysiology, classification and available guidelines of acute pancreatitis. Turk J Gastroenterol 25: 351-357, 2014.
4. Yadav D, O'Connell M and Papachristou GI: Natural history following the first attack of acute pancreatitis. Am J Gastroenterol 107: 1096-1103, 2012.
5. Gillies N, Pendharkar SA, Asrani VM, Mathew J, Windsor JA and Petrov MS: Interleukin-6 is associated with chronic hyperglycemia and insulin resistance in patients after acute pancreatitis. Pancreatology 16: 748-755, 2016.
6. Kambhampati S, Park W and Habtezion A: Pharmacologic therapy for acute pancreatitis. World J Gastroenterol 20: 16868-16880, 2014.
7. Hegazi RA and DeWitt T: Enteral nutrition and immune modulation of acute pancreatitis. World J Gastroenterol 20: 16101-16105, 2014.

8. Banks PA, Bollen TL, Dervenis C, Gooszen HG, Johnson CD, Sarr MG, Tsiotos GG and Vege SS; Acute Pancreatitis Classification Working Group: Classification of acute pancreatitis-2012: Revision of the Atlanta classification and definitions by international consensus. Gut 62: 102-111, 2013.
9. Zerem E: Treatment of severe acute pancreatitis and its complications. World J Gastroenterol 20: 13879-13892, 2014.
10. Caserta S, Mengozzi M, Kern F, Newbury SF, Ghezzi P and Llewelyn MJ: Severity of systemic inflammatory response syndrome affects the blood levels of circulating inflammatory-relevant MicroRNAs. Front Immunol 8: 1977, 2018.
11. Hoque R, Malik AF, Gorelick F and Mehal WZ: Sterile inflammatory response in acute pancreatitis. Pancreas 41: 353-357, 2012.
12. Giuliani AL, Sarti AC, Falzoni S and Di Virgilio F: The P2X7 receptor-interleukin-1 liaison. Front Pharmacol 8: 123, 2017.
13. Zhang GX, Wang MX, Nie W, Liu DW, Zhang Y and Liu HB: P2X7R blockade prevents NLRP3 inflammasome activation and pancreatic fibrosis in a mouse model of chronic pancreatitis. Pancreas 46: 1327-1335, 2017.
14. Liu PY, Lee IH, Tan PH, Wang YP, Tsai CF, Lin HC, Lee FY and Lu CL: P2X7 receptor mediates spinal microglia activation of visceral hyperalgesia in a rat model of chronic pancreatitis. Cell Mol Gastroenterol Hepatol 1: 710-720.e5, 2015.
15. Dong X, Fu J, Yin X, Cao S, Li X, Lin L; Huyiligeqi and Ni J: Emodin: A review of its pharmacology, toxicity and pharmacokinetics. Phytother Res 30: 1207-1218, 2016.
16. Jiang CG: The treatment of acute pancreatitis with Dachengqi decoction in 32 cases. Zhongguo Wei Zhong Bing Ji Jiu Yi Xue 22: 249, 2010 (In Chinese).
17. Yang DY, Duan SB and Aili JT: Effect of qingyi decoction in treating severe acute pancreatitis and its impacts on blood level of tumor necrosis factor-alpha, interleukin-6 and inteleukin-8. Zhongguo Zhong Xi Yi Jie He Za Zhi 29: 1122-1124, 2009 (In Chinese).
18. Wu L, Cai B, Zheng S, Liu X, Cai H and Li H: Effect of emodin on endoplasmic reticulum stress in rats with severe acute pancreatitis. Inflammation 36: 1020-1029, 2013.
19. Xia XM, Li BK, Xing SM and Ruan HL: Emodin promoted pancreatic claudin-5 and occludin expression in experimental acute pancreatitis rats. World J Gastroenterol 18: 2132-2139, 2012.
20. Liu L, Zou J, Liu X, Jiang LH and Li J: Inhibition of ATP-induced macrophage death by emodin via antagonizing P2X7 receptor. Eur J Pharmacol 640: 15-19, 2010.
21. Zhu T, Zhang L, Ling S, Duan J, Qian F, Li Y and Xu JW: Scropolioside B inhibits IL-1β and cytokines expression through NF-κB and inflammasome NLRP3 pathways. Mediators Inflamm 2014: 819053, 2014.
22. Rodgers MA, Bowman JW, Fujita H, Orazio N, Shi M, Liang Q, Amatya R, Kelly TJ, Iwai K, Ting J, *et al*: The linear ubiquitin assembly complex (LUBAC) is essential for NLRP3 inflammasome activation. J Exp Med 211: 1333-1347, 2014.
23. Han JW, Shim DW, Shin WY, Heo KH, Kwak SB, Sim EJ, Jeong JH, Kang TB and Lee KH: Anti-inflammatory effect of emodin via attenuation of NLRP3 inflammasome activation. Int J Mol Sci 16: 8102-8109, 2015.
24. Xiang H, Wang G, Qu J, Xia S, Tao X, Qi B, Zhang Q and Shang D: Yin-chen-hao tang attenuates severe acute pancreatitis in rat: An experimental verification of in silico network target prediction. Front Pharmacol 7: 378, 2016.
25. Cen Y, Liu C, Li X, Yan Z, Kuang M, Su Y, Pan X, Qin R, Liu X, Zheng J, *et al*: Artesunate ameliorates severe acute pancreatitis (SAP) in rats by inhibiting expression of pro-inflammatory cytokines and Toll-like receptor 4. Int Immunopharmacol 38: 252-260, 2016.
26. Tukaj C, Olewniak-Adamowska A, Pirski MI and Woźniak M: Ultrastructural aspects of acute pancreatitis induced by 2, 2'-azobis (2-amidinopropane) dihydrochloride (AAPH) in rats. Folia Morphol 71: 136-141, 2012.
27. Zhang XP, Li ZF, Liu XG, Wu YT, Wang JX, Wang KM and Zhou YF: Effects of emodin and baicalein on rats with severe acute pancreatitis. World J Gastroenterol 11: 2095-2100, 2005.
28. Sanz JM, Chiozzi P, Ferrari D, Colaianna M, Idzko M, Falzoni S, Fellin R, Trabace L and Di Virgilio F: Activation of microglia by amyloid {beta} requires P2X7 receptor expression. J Immunol 7: 4378-4385, 2009.
29. Zhu S, Wang Y, Wang X, Li J and Hu F: Emodin inhibits ATP-induced IL-1β secretion, ROS production and phagocytosis attenuation in rat peritoneal macrophages via antagonizing P2X7 receptor. Pharm Biol 52: 51-57, 2014.
30. Xu H, Xiong C, He L, Wu B, Peng L, Cheng Y, Jiang F, Tan L, Tang L, Tu Y, *et al*: Trans-resveratrol attenuates high fatty acid-induced P2X7 receptor expression and IL-6 release in PC12 cells: Possible role of P38 MAPK pathway. Inflammation 38: 327-337, 2015.
31. Chen Q, Wu H, Qin S, Liu C, Chen Y, Yang Y and Xu C: The P2X7 receptor involved in gp120-induced cell injury in BV2 Microglia. Inflammation 39: 1814-1826, 2016.
32. Albalawi F, Lu W, Beckel JM, Lim JC, McCaughey SA and Mitchell CH: The P2X7 receptor primes IL-1β and the NLRP3 inflammasome in astrocytes exposed to mechanical strain. Front Cell Neurosci 11: 227, 2017.
33. Yue N, Huang H, Zhu X, Han Q, Wang Y, Li B, Liu Q, Wu G, Zhang Y and Yu J: Activation of P2X7 receptor and NLRP3 inflammasome assembly in hippocampal glial cells mediates chronic stress-induced depressive-like behaviors. J Neuroinflammation 10: 102, 2017.
34. Martinon F, Burns K and Tschopp J: The inflammasome: A molecular platform triggering activation of inflammatory caspases and processing of proIL-beta. Mol Cell 10: 417-426, 2002.
35. Yan Y, Jiang W, Liu L, Wang X, Ding C, Tian Z and Zhou R: Dopamine controls systemic inflammation through inhibition of NLRP3 inflammasome. Cell 160: 62-73, 2015.
36. Slowik A, Lammerding L, Zendedel A, Habib P and Beyer C: Impact of steroid hormones E2 and P on the NLRP3/ASC/Casp1 axis in primary mouse astroglia and BV-2 cells after in vitro hypoxia. J Steroid Biochem Mol Biol 183: 18-26, 2018.
37. Li X and Zhong F: Nickel induces interleukin-1β secretion via the NLRP3-ASC-caspase-1 pathway. Inflammation 37: 457-466, 2014.
38. Zhang A, Pan W, Lv J and Wu H: Protective effect of amygdalin on LPS-induced acute lung injury by inhibiting NF-κB and NLRP3 signaling pathways. Inflammation 40: 745-751, 2017.
39. Hansen MR, Krabbe S and Novak I: Purinergic receptors and calcium signalling in human pancreatic duct cell lines. Cell Physiol Biochem 22: 157-168, 2008.
40. Novak I, Nitschke R and Amstrup J: Purinergic receptors have different effects in rat exocrine pancreas. Calcium signals monitored by fura-2 using confocal microscopy. Cell Physiol Biochem 12: 83-92, 2002.
41. Lu G, Tong Z, Ding Y, Liu J, Pan Y, Gao L, Tu J, Wang Y, Liu G and Li W: Aspirin protects against acinar cells necrosis in severe acute pancreatitis in mice. Biomed Res Int 2016: 6089430, 2016.
42. Novak I, Jans IM and Wohlfahrt L: Effect of $P2X_7$ receptor knockout on exocrine secretion of pancreas, salivary glands and lacrimal glands. J Physiol 588: 3615-3627, 2010.
43. Schroder K and Tschopp J: The inflammasomes. Cell 140: 821-832, 2010.
44. de Torre-Minguela C, Mesa Del Castillo P and Pelegrín P: The NLRP3 and pyrin inflammasomes: Implications in the pathophysiology of autoinflammatory diseases. Front Immunol 8: 43, 2017.
45. Gunjaca I, Zunic J, Gunjaca M and Kovac Z: Circulating cytokine levels in acute pancreatitis-model of SIRS/CARS can help in the clinical assessment of disease severity. Inflammation 35: 758-763, 2012.
46. Wang XY, Tang QQ, Zhang JL, Fang MY and Li YX: Effect of SB203580 on pathologic change of pancreatic tissue and expression of TNF-α and IL-1β in rats with severe acute pancreatitis. Eur Rev Med Pharmacol Sci 18: 338-343, 2014.
47. Wen H, Miao EA and Ting JP: Mechanisms of NOD-like receptor-associated inflammasome activation. Immunity 39: 432-441, 2013.
48. Xu MH, Yuan FL, Wang SJ, Xu HY, Li CW and Tong X: Association of interleukin-18 and asthma. Inflammation 40: 324-327, 2017.
49. Xiang H, Tao X, Xia S, Qu J, Song H, Liu J and Shang D: Emodin alleviates sodium taurocholate-induced pancreatic acinar cell injury via MicroRNA-30a-5p-mediated inhibition of high-temperature requirement A/Transforming growth factor beta 1 inflammatory signaling. Front Immunol 8: 1488, 2017.